Annals of Clinical Case Reports

Research Article
Published: 20 Dec, 2021

Using Multi-Model Diffusion Weighted Imaging to Study the Diagnostic Value and Severity of Acute Kidney Injury in Severe Acute Pancreatitis

*Xinghui Li[1#], Qi Liang[2#], Zenghui Li[1], Yong Li[1], Yifan Ji[1], Tianwu Chen[1] and Xiao-Ming Zhang[1]**

[1]Sichuan Key Laboratory of Medical Imaging, Department of Radiology, Affiliated Hospital of North Sichuan Medical College, China

[2]Department of Laboratory, Affiliated Hospital of North Sichuan Medical College, China

[#]These authors contributed equally to this work

Abstract

Objective: To explore the diagnostic value and severity of Acute Kidney Injury (AKI) in patients with Severe Acute Pancreatitis (SAP) using Intravoxel Incoherent Motion Imaging (IVIM), Diffusion Tensor Imaging (DTI) and Diffusion Kurtosis Imaging (DKI).

Methods: Fifty-six SAP patients were divided into an AKI group and a non-AKI group. All patients underwent routine abdominal, IVIM, DTI and DKI scans, and the main MRI parameters of kidney and clinical characteristics were measured. The diagnostic performance of AKI was compared, and the relationships among these indices, Glomerular Filtration Rate (eGFR) and AKI staging were analyzed. Finally, all parameters were analyzed by single- and multiparameter regression.

Results: Compared with the non-AKI group, the percentage of CD3+ CD4+ T cells and $CD4^+/CD8^+$ ratio in peripheral blood increased significantly. The fast ADC value and Ff ADC value of the renal medulla in the AKI group were significantly lower than those in the non-AKI group. The FA value in the renal cortex was significantly lower than that in the medulla and significantly lower than that in the non-AKI group. The renal medulla MK value in the AKI group was significantly lower than that of the non-AKI group and had the best diagnostic value for AKI in SAP patients, which was positively correlated with AKI staging and negatively correlated with the eGFR. MK values, the percentage of CD3+ CD4+ T cells and $CD4^+/CD8^+$ ratio were independent risk factors for AKI by multiparameter logistic regression analysis.

Conclusion: The measurement of renal DKI parameters combined with $CD4^+$ T lymphocytes is practical for early diagnosis and predicting the severity of renal injury in SAP patients.

Keywords: Acute severe pancreatitis; Acute kidney injury; Intravoxel incoherent motion imaging; Diffusion tensor imaging; Diffusion kurtosis imaging

OPEN ACCESS

***Correspondence:**
Xiao-Ming Zhang, Sichuan Key Laboratory of Medical Imaging, Department of Radiology, Affiliated Hospital of North Sichuan Medical College, Nanchong 637000, China, Tel: +86-817-2262218; Fax: +86-817-2222856;
E-mail: cjr.zhxm@vip.163.com

Received Date: *18 Nov 2021*
Accepted Date*: 03 Dec 2021*
Published Date*: 20 Dec 2021*

Citation:
Li X, Liang Q, Li Z, Li Y, Ji Y, Chen T, et al. Using Multi-Model Diffusion Weighted Imaging to Study the Diagnostic Value and Severity of Acute Kidney Injury in Severe Acute Pancreatitis. Ann Clin Case Rep. 2021; 6: 2064.

ISSN: 2474-1655

Introduction

Acute Pancreatitis (AP) is a systemic disease with immune disorders, especially Severe Acute Pancreatitis (SAP). Acute Kidney Injury (AKI) is a common complication in hospitalized patients and manifests as a sudden decrease in renal excretion. The mortality rate can be as high as 70% when AP is combined with AKI [1-4]. However, the onset of AP-induced renal injury is insidious, and its early clinical manifestations are nonspecific. The levels of serum Creatinine (sCr) and Blood Urea Nitrogen (BUN) indicators may be normal, while renal lesions are still in a reversible stage, and active treatment can reduce or delay the occurrence of renal injury [5-7]. Therefore, early detection of AP kidney injury and understanding its immune mechanism can delay the occurrence and development of AP kidney injury, which are of great significance to improve the cure rate and reduce mortality [8]. T lymphocyte subsets participate in the formation of the body's immune system, which mainly maintains the body's immune balance through the T cell network of helper T cells, namely CD4+ T cells and suppressor T cells, namely CD8+ T cells.

In recent years, functional kidney MR imaging has developed rapidly, making it possible to noninvasively evaluate the morphology and function of the kidney [9,10]. With the continuous improvement of biological tissue diffusion technology, the IVIM two-compartment model was first

proposed by Bihan et al. [11], which measures the microcirculation perfusion and diffusion of the kidney through the observed signal attenuation at different B values. Therefore, IVIM has shown great potential in the diagnosis and evaluation of kidney diseases by revealing the pathophysiological changes of the disease. DTI indirectly reflects information on kidney function changes by detecting the degree and direction of limited diffusion movement of water molecules in human tissues [12]. With the extensive application of parallel acquisition technology and plane echo imaging, the application of DTI in organs other than the central nervous system is expanding and becoming a hot topic [13,14]. In addition, the kidney is characterized by high perfusion, high water content and radial arrangement of various structures (renal tubules, collecting ducts, and blood vessels), which lays a theoretical foundation for renal DTI imaging. DKI was derived from DTI model. Due to the impediment of cell membranes, compartments and special cell morphological changes in the lesion area, water molecule diffusion does not always follow a Gaussian distribution. The newly developed DKI was employed to describe the non-Gaussian distribution. Kurtosis, as a dimensionless metric, was employed to quantify the degree of non-Gaussian diffusion and characterize tissue heterogeneity [9,15-17]. At present, some scholars use a 3.0 T MRI scanner to study kidney DKI in healthy volunteers, and they have confirmed its application value in the kidney [18-20]. As DKI is a newly developed functional imaging technology, there are no reports on the evaluation of renal function in AP patients.

In addition, our previous clinical studies have confirmed the value of DTI in the quantitative diagnosis and severity evaluation of AP [14]. Therefore, we applied the above imaging techniques to further explore the early diagnostic value and severity classification of acute kidney injury in SAP patients, as well as the change of T lymphocyte subsets.

Materials and Methods

Patient population

The study was approved by the ethics committee of the Affiliated Hospital of North Sichuan Medical College, and all participants signed informed consent forms. Consecutive patients with a clinical history of SAP in our institute between January 2017 and June 2020 were initially considered in this study. SAP diagnosis was based on the Atlanta classification criteria revised in 2012 and is presented in Table 1 [21]. The diagnosis of organ failure was performed using the modified Marshall scoring system [22], as shown in Table 2, which included the respiratory, circulatory and urinary systems. Organ failure could be diagnosed if any of the three systems reached 2 points or more. Local complications could be aseptic or bacterial within 4 weeks and after 4 weeks. Systemic complications refer to basic diseases (such as coronary heart disease) aggravated by the exacerbation of AP [22]. Patients with chronic pancreatitis, tumor and chronic liver disease, chronic renal disease, hypoproteinemia, severe systemic infection or hemorrhagic disease, and poor compliance in MR examination were excluded.

All patients were divided into AKI and non-AKI groups according to serum creatinine levels. The AKI diagnostic and grading criteria conformed to the 2012 guidelines for improving the prognostic organization (KDIGO) of global kidney disease [23]. The diagnostic criteria were as follows: (1) Serum creatinine increased more than 26.5 μmol/L within 48 h, (2) serum creatinine levels increased by 1.5 times over the baseline within 7 days; and (3) the urine volume in six consecutive hours was less than 5 mL/kg/h. The AKI staging criteria are detailed in Table 3. All patients completed the determination of serum creatinine levels one day before the MRI examination. The formula for calculating the eGFR based on the epidemiological collaboration (CKD-EPI) for chronic kidney disease is as follows [24]:

Female: Cr ≤ 0.7 mg/dl, $GFR = 144 \times \left(Cr/0.7\right)^{0.329} \times 0.993^{age}$

Cr<0.7 mg/dl, $GFR = 144 \times \left(Cr/0.7\right)^{1.209} \times 0.993^{age}$

Male: Cr ≤ 0.9 mg/dl, $GFR = 141 \times \left(Cr/0.9\right)^{0.411} \times 0.993^{age}$

Cr>0.9 mg/dl, $GFR = 141 \times \left(Cr/0.9\right)^{1.209} \times 0.993^{age}$

MR technologies

All subjects were scanned in the supine position on a 3.0T MRI scanner (Discovery MR 750; GE Medical Systems, Milwaukee, WI.) with a 50 mT/m maximum gradient length and 200 T/m/s maximum slew rate using a 32-channel body array coil with sixteen anterior and sixteen posterior elements [14]. The routine scan sequence included transverse T1WI, T2WI, coronal T2WI and three-phase dynamic enhancement scans covering the two kidneys. To avoid increasing the burden on the kidneys, AP patients with abnormal renal function did not receive enhanced MR scans. Details of the scanning parameters

Table 1: Classification criteria for acute pancreatitis in Atlanta 2012.

Severity	Definition
Mild	No organ failure, no local or systemic complications
Moderate	Organ failure time <48 h or the existence of local and systemic complications
Severe	Organ failure time >48 h

Table 2: Improved Marshall scoring system.

Organ system	0 point	1 point	2 points	3 points	4 points
Respiration (PaO2/FiO2)	>400	301-400	201-300	101-200	≤ 101
Kidney (serum creatinine)	≤ 134	134-169	170-310	311-439	>439
Cardiovascular (systolic pressure)	>90	<90, reaction during infusion	<90, no reaction during infusion	<90, PH<7.3	<90, PH<7.2

Table 3: AKI staging criteria.

Staging	Serum creatinine	Urinary volume
I	1.5-1.9 times of the base value or increase ≥ 26.5 umol/L	<0.5 ml/kg/h duration 6-12 h
II	2.0-2.9 times the base value	<0.5 ml/kg/h duration over 12 h
III	Start renal replacement therapy or 3 times base value or creatinine ≥ umol/L 353.6	<0.3 ml/kg/h duration over 24 h or anuria duration over 12 h

Table 4: Sequences and parameters of the 3.0T MRI scan of the upper abdomen.

	TR (ms)	TE (ms)	Flip angle	Thickness (mm)	Gap (mm)	Matrix	FOV (cm)
AX 3D LAVA-Flex	4.2	2.6/1.3	15-20°	5	0	384 × 224	26–33
AX FRFSE T2WI	10000-12000	90-100	90°	5	0.5	256 × 192	36 × 34
COR SSFSE T2WI	2500-3500	80-100	90°	5	0.5	384 × 256	39 × 33
AX SSFSE T2WI	2500-3500	80-100	90°	5	0.5	320 × 256	39 × 33
MRCP	3045	1300	90°	40	40-50	384 × 224	32 × 34
AX 3D LAVA C+*	4.2	2.6/1.3	15-20°	5	0	384 × 224	26-33

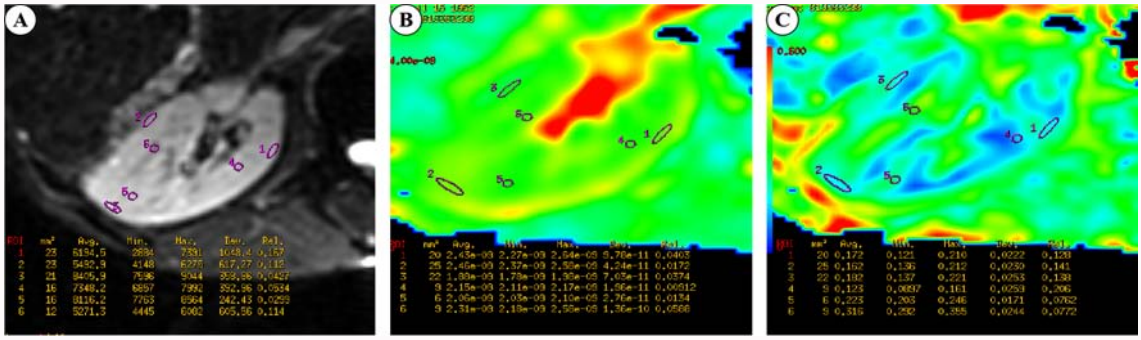

Figure 1: ROI placement of the kidney cortex and medulla on DTI: signal intensity image (A), ADC map (B), FA map (C).

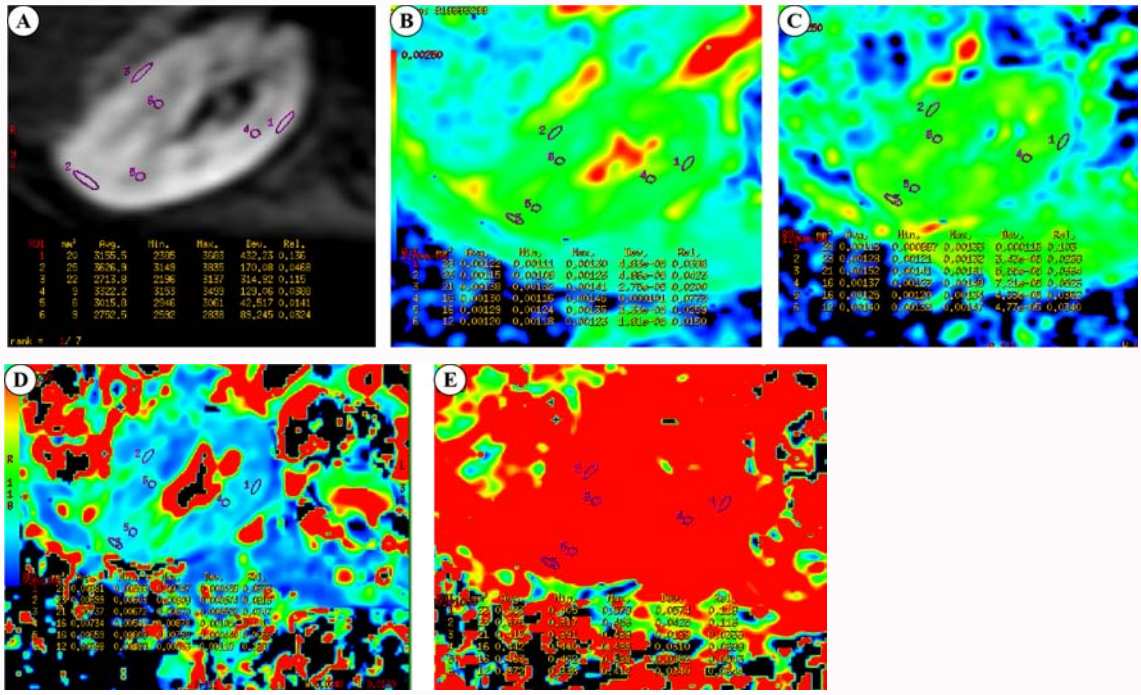

Figure 2: ROI placement of the kidney cortex and medulla on IVIM: Signal intensity image (A), standard ADC map (B), slow ADC map (C), fast ADC map (D), and Ff ADC map (E).

are shown in Table 4 [14]. The patient fasted without water for 6 hours prior to MR examination.

Breath-holding DTI and free-breathing IVIM and DKI scans of the kidneys were performed in the transverse position before enhanced scanning. The DTI parameters were as follows: TR 2500 ms, TE minimum ms, section thickness =5 mm, intersection gap =0 mm, FOV= 28 cm to 36 cm, bandwidth 250 Hz, NEX=1 and matrix = 256 × 192. Auto shim: on, diffusion-encoding directions =9, b-value =500 s/mm^2. The IVIM and DKI sequences were both based on single shot DW spin echo planar imaging with a fat-suppressed sequence, and the IVIM-specific parameters were as follows: b-factor values (0, 50, 100, 150, 200, 300, 500, 800, 1000 and 1500 s/mm^2), TR/TE= 4000 ms to 4500 ms/90 ms to 100 ms, matrix = 192~256 × 192~256, FOV= 28 cm to 36 cm, section thickness =5 mm, and intersection gap =0 mm. The DKI parameters were as follows: b-factor values (0, 1000, 2000 s/mm^2), diffusion-encoding directions =30, TR 8000 ms, TE minimum ms, thickness =5 mm, intersection gap =0 mm, NEX=2. The average scan times of DTI, IVIM and DKI were 21 sec, 2 min to 3

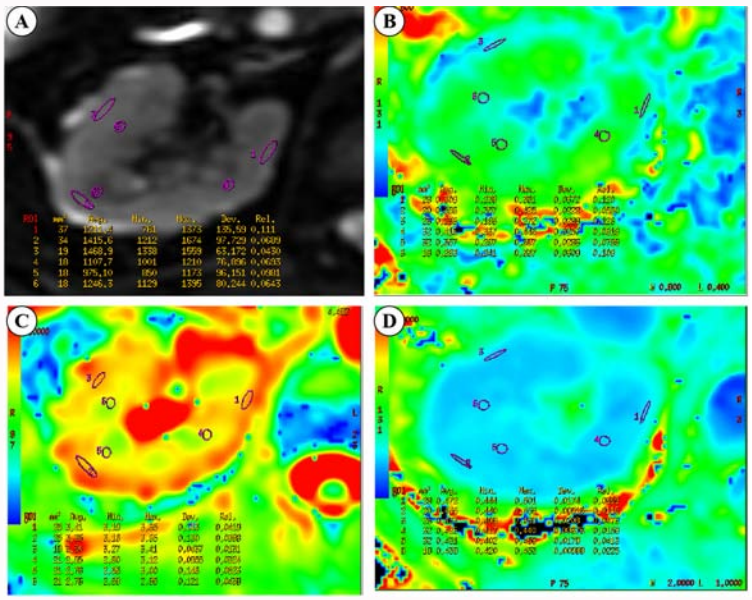

Figure 3: ROI placement of the kidney cortex and medulla on a DKI image: Signal intensity image (A), FA map (B), MD map (C), and MK map (D).

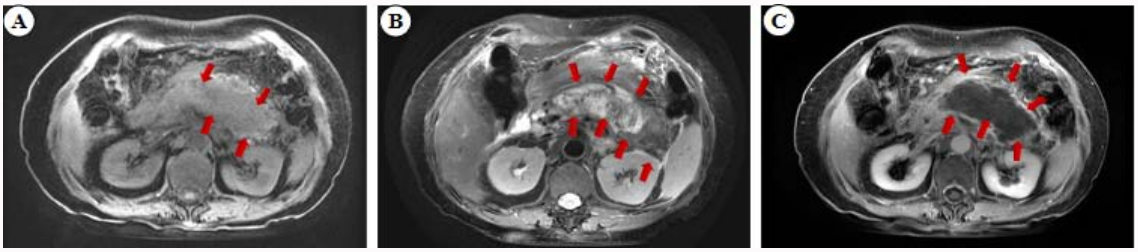

Figure 4: A 63-year-old man with non-AKI SAP. Fat suppression Lava-flex T1 (A), FRFSE T2 (B) weighted images and contrast Lava-flex T1 (C) show a well-marginated necrotic area without enhancement located in the whole pancreatic tissue (arrow). The serum creatinine, urea nitrogen, uric acid and eGFR were 87.3 μmol/L, 6.39 mmol/L, 339.1 μmol/L, and 107.4 mL/min, respectively.

min and 3 min to 4 min, respectively.

MR image analysis

The original DTI, IVIM-DWI, and DKI images were loaded onto a workstation (Advantage Workstation 4.4; GE Healthcare). The FuncTool 2 software package was used to process all raw data, and maps of the corresponding parameters were then obtained by automatic pixel-wise analysis on the GE workstation [25]. Images of the surrounding fat, bone, gas and other tissue were removed by applying the threshold definition method. The parameters of the renal cortex and medulla were quantitatively measured, including DTI-associated ADC, Fractional Anisotropy (FA), IVIM-associated standard ADC, perfusion fraction (Ff ADC), pseudodiffusion coefficient (fast ADC), diffusion coefficient (slow ADC), DKI-associated Mean Kurtosis (MK), mean corrected diffusion coefficient (MD) and FA value.

To avoid the effect of cardiac motion on the image, the right kidney was selected as the target Region of Interest (ROI). Renal ROIs were manually delineated on the b=0 DW images with the aid of T2-weighted images as a reference for distinguishing the cortex and medulla. In each kidney, the ROI of the renal cortex and medulla was an irregular area with a size of 15 ± 2 mm^2 and contained at least 10 to 15 pixels. ROIs were manually drawn at the level of the renal hilum carefully avoiding artifacts, the kidney collection system, and the edge of the kidney. Then, the measurement was repeated three times, and the average values were recorded (Figures 1-3). All parameters were measured by a radiologist with more than five years of experience in abdominal MR. After 3 days, the second time was measured by the same method, and the results were averaged as the final results of statistical analyses.

Laboratory biochemical tests

Biochemical laboratory indicators were determined by an automatic biochemical analyzer (Mindray BS-22) according to the operation procedure and carried out by special personnel in the laboratory of our hospital. These indicators included serum Creatinine (sCr), Blood Urea Nitrogen (BUN), Serum Uric Acid (UA), Serum Cystatin C (Cys-C), Fasting Blood Glucose (FBG), Serum Amylase (AMY), Serum Lipase (LIP), Serum Cholinesterase (CHE), Total Protein (TP), Albumin (ALB), Globulin (GLOB), Total Bilirubin (TBIL), Direct Bilirubin (DBIL), Total Bile Acid (TBA), Glutamate-Propionate Aminotransferase (ALT), Glutamate-Oxalate Aminotransferase (AST), R Glutamate Transferase (GGT) and Alkaline Phosphatase (ALP).

$CD4^+$, $CD8^+$ T cell subgroup detection

Peripheral blood lymphocyte counts were analyzed by flow cytometry (Mindray BriCyte E6, Shenzhen) and supporting reagents to detect specific fluorescent antibodies on the surface of immune

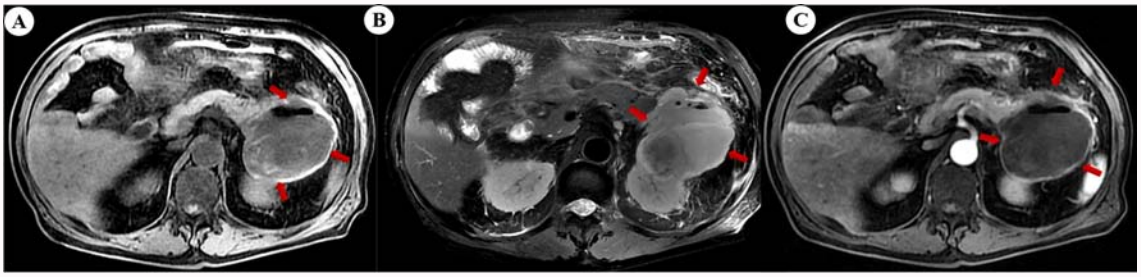

Figure 5: A 67-year-old man with stage II AKI SAP. Fat suppression Lava-flex T1 (A), FRFSE T2 (B) weighted images and contrast Lava-flex T1 (C) show a necrotic area without enhancement located in the pancreatic tail and pyogenic infection in the left perirenal space (arrow). The serum creatinine, urea nitrogen, uric acid and eGFR were 340.6 μmol/L, 21.6 mmol/L, 343.7 μmol/L, and 65.4 ml/min, respectively.

cells. The specific operation was strictly in accordance with the kit instructions and performed by a dedicated person in the laboratory of our hospital. The percentages of total T lymphocytes ($CD3^+$), Th lymphocytes ($CD3^+$ $CD4^+$) and Ts lymphocytes ($CD3^+$ $CD8^+$) were reported, as well as the $CD4^+/CD8^+$ ratio.

Statistical analysis

Continuous variables were tested for normality, and normally distributed variables were expressed as the means ± standard deviation. The classification variables were represented by the composition ratio. Multiple independent samples t tests were used to compare the differences in MR parameter values between the two groups. Spearman correlation analysis was used to evaluate the correlation between renal parenchymal parameters and eGFR and renal injury grade. Chi-square test was used for classification variables. A Receiver Operating Characteristic (ROC) curve was established to analyze the diagnostic efficacy of IVIM, DTI, and DKI. Univariate and multivariate regression analyses were used to predict the risk factors for AKI. All statistical analyses were performed using Statistical Package for Social Sciences (SPSS) for Windows (Version 13.0, Chicago, IL, USA). $P<0.05$ was considered to be significant.

Results

General information of SAP patients

In total, 68 patients were included in the study, and 12 patients were excluded (1 with chronic pancreatitis, 2 with tumor and chronic liver disease, 3 with chronic renal disease or renal failure, 2 with hypoproteinemia, 2 with severe systemic infection or hemorrhagic disease, and 2 with poor compliance in MR examination). The final study group consisted of 56 consecutive patients with SAP, including 21 women and 35 men with an average age of 59.2 ± 15.9 years (20 to 81 years), 14 of whom were diagnosed with AKI according to the KDIGO criteria (Figure 4, 5). The number of AKI patients with stage I, II, and III disease was 7, 5, and 2, accounting for 50%, 36%, and 14%, respectively. The proportion of men was higher than that of women (28.6% *vs.* 19.0%, $P<0.05$). The basic information of all patients is shown in Table 5. The indicators were not significantly different between the AKI and non-AKI groups, which included age ($P=0.732$), FBG ($P=0.421$), AMY ($P=0.219$), TP ($P=0.080$), ALB ($P=0.057$), GLOB ($P=0.286$), TBIL ($P=0.473$), DBIL ($P=0.225$), TBA ($P=0.226$), ALT ($P=0.876$), AST ($P=0.432$), GGT ($P=0.722$) and ALP ($P=0.560$). Compared with the non-AKI group, the blood urea nitrogen, creatinine and uric acid were significantly increased in the AKI group, while the blood LIP, CHE and estimated Glomerular Filtration Rate (eGFR) were significantly decreased ($P<0.05$).

Comparison of T lymphocyte subsets

The changes in T lymphocyte subsets in peripheral blood in both groups are shown in Table 6. The percentage of CD3+ CD4+ T cells and CD4+/CD8+ ratio of peripheral blood in the AKI group were significantly lower than those in the non-AKI group ($P<0.05$). Although the percentages of CD3+ and CD3+ CD8+ T cells in the AKI group were also lower than those in the non-AKI group, the differences were not statistically significant (P>0.05).

Analysis of IVIM, DTI, and DKI parameters

No serious artifacts were found in the MR images of any of the subjects. The results of the main renal IVIM, DTI and DKI parameters in both groups are shown in Tables 7-9, respectively. In IVIM mode, the fast ADC and Ff ADC of the renal medulla in the AKI group were lower than those in the non-AKI group ($P=0.043$; 0.037). The slow ADC values in the renal cortex and medulla were not significantly different between the AKI and non-AKI groups ($P>0.05$). In DTI mode, the FA value of the renal cortex in both groups was lower than that in the medulla ($P=0.013$; 0.041), and the FA value of the renal cortex and medulla in the AKI group was significantly lower than that in the non-AKI group ($P=0.419$; 0.026). However, there was no significant difference in ADC values between the renal cortex and medulla ($P=0.438$; 0.429). In addition, the renal cortex FA value in the AKI group was significantly lower than that in the non-AKI control group ($P=0.045$), and there were no significant differences between renal cortex ADC and medullary ADC in the two groups ($P=0.331$; 0.349). In DKI mode, the MK value of the medulla was higher than that of the cortex ($P=0.045$), and the MK value in the AKI group was also higher than that in the non-AKI group ($P=0.041$).

Comparison of the diagnostic efficacy of IVIM, DTI, and DKI in the diagnosis of AKI

To further explore the diagnostic efficacy of positive parameters for AKI, a Receiver Operating Characteristic (ROC) curve was established by taking the AKI group as the positive sample, and the analyzed indices were divided into several segments according to the numerical range of the total level of the sample (broken line). According to the ROC analysis, the above five indicators have high diagnostic value, as shown in Table 10 and Figure 6. However, MK of the medulla had the highest diagnostic efficiency, and its sensitivity, specificity, and Youden index were 0.793, 0.818, and 0.611, respectively.

Correlation analysis

To further analyze the relationship between each parameter and eGFR, we performed a Spearman correlation test on AKI patients. The results showed that eGFR was positively correlated with IVIM-

Table 5: Comparison of general clinical data.

Clinical index	non-AKI (n=42)	AKI (n=14)	*P*
Age	58.65 ± 15.62	60.83 ± 13.68	0.732
Gender (female/male)	118/24	4/10	0.039
Bun (mmol/L)	6.02 ± 2.85	16.41 ± 8.43	<0.001
Cr (μmol/L)	75.57 ± 23.97	358.37 ± 266.33	<0.001
UA (μmol/L)	292.03 ± 102.65	383.94 ± 171.58	0.025
eGFR(ml/min)	108.67 ± 20.34	82.45 ± 21.37	<0.01
FBG (mmol/L	7.70 ± 3.22	7.23 ± 3.86	0.421
AMY (U/L)	852.77 ± 507.00	869.33 ± 872.52	0.219
LIP (U/L)	803.77 ± 518.69	719.80 ± 947.56	0.037
CHE (U/L)	6675.78 ± 1921.20	4685.22 ± 1874.63	<0.001
TP (g/L)	63.47 ± 6.29	58.52 ± 9.52	0.080
ALB (g/L)	37.08 ± 4.64	33.63 ± 6.68	0.057
GLOB (g/L)	26.66 ± 5.23	24.88 ± 6.23	0.286
TBIL (μmol/L	40.65 ± 46.44	31.34 ± 26.51	0.472
DBIL (μmol/L	19.69 ± 28.84	12.17 ± 14.99	0.224
TBA (μmol/L	34.45 ± 69.10	13.15 ± 22.82	0.225
ALT (U/L)	168.13 ± 188.50	172.39 ± 226.09	0.866
AST (U/L)	147.65 ± 209.97	110.83 ± 140.16	0.432
GGT (U/L)	271.03 ± 316.83	270.00 ± 251.27	0.711
ALP (U/L)	130.31 ± 99.02	134.33 ± 93.97	0.550

Table 6: Comparison of T lymphocyte subsets between AKI and non-AKI groups.

T cell	non-AKI (n=42)	AKI (n=14)	*t*	*P*
CD3+(%)	62.23 ± 15.19	53.83 ± 11.82	0.98	0.076
CD3+CD4+(%)	41.78 ± 10.45	27.81 ± 8.44	2.34	0.021*
CD3+CD8+(%)	22.13 ± 5.69	24.73 ± 6.62	0.29	0.460
CD4+/CD8+	1.72 ± 0.36	1.21 ± 0.29	1.95	0.043*

*represents *P*<0.05

Table 7: Comparative analysis of renal IVIM parameters in the AKI group and non-AKI group.

	slow ADC		fast ADC		Ff ADC	
Group	Cortex	Medulla	Cortex	Medulla	Cortex	Medulla
Non-AKI	1.34 ± 0.21	1.26 ± 0.25	22.71 ± 2.38	17.25 ± 1.25[a]	0.42 ± 0.05	0.25 ± 0.02
AKI	1.35 ± 0.24	1.33 ± 0.28	20.63 ± 2.87	16.86 ± 1.12[a,b]	0.38 ± 0.03[b]	0.22±0.02[a,b]

[a]Represents *P*<0.05 compared with the cortex by t test; b represents *P*<0.05 compared with the non-AKI group by t test.

Table 8: Comparative analysis of renal DTI parameters in the AKI group and non-AKI.

	FA		ADC	
Group	Cortex	Medulla	Cortex	Medulla
Non-AKI	0.28±0.02	0.57±0.17[a]	2.24±0.17	2.20±0.19
AKI	0.23±0.05[b]	0.41±0.16[a,b]	2.16±0.29	2.12±0.28

[a]Represents *P*<0.05 compared with the cortex by t test; b represents *P*<0.05 compared with the non-AKI group by t test

fast ADC value, DTI-FA value, CD4+/CD8+ ratio and $CD3^+$ $CD4^+$ T cell percentage (fast ADC of medulla: r=0.513, *P*=0.012; fast ADC of cortex: r=0.548, *P*=0.009; medulla FA: r=0.40, *P*=0.016; cortex FA: r=0.36, *P*=0.021; $CD4^+/CD8^+$ ratio: r=0.45, *P*=0.014; $CD3^+$ $CD4^+$ T cell percentage: r=0.507, *P*=0.011), and it had a highly negative correlation with the MK value (medulla MK: r= -0.882, *P*=0.000). Since the MK value had the highest correlation with eGFR (Figure 6), we further grouped the AKI patients according to the stages of AKI and compared the MK differences among different stages of AKI patients. The comparison between groups showed that there were significant differences in renal medulla MK values among patients with different AKI stages (F=46.09, *P*=0.000), MK values increased with increasing AKI stage (Figure 3, 7), and there was a positive correlation between renal medulla MK values and AKI stage (r=0.789, *P*=0.000). We found that there were significant differences in renal medulla MK values among patients with different AKI stages (F=46.09, *P*=0.000). As the AKI stage increased, the MK value showed an increasing trend (Figure 3, 7), and the renal medulla MK value was positively correlated with the AKI stage (r=0.789, *P*=0.000).

Table 9: Comparative analysis of renal DKI parameters in the AKI group and non-AKI group.

	FA		MK		MD	
Group	Cortex	Medulla	Group	Group	Group	Group
Non-AKI	0.22 ± 0.04	0.26 ± 0.03	0.40 ± 0.03	0.42 ± 0.02[a]	2.67 ± 0.34	2.42 ± 0.26
AKI	0.21 ± 0.04	0.24 ± 0.05	0.41 ± 0.07	0.49 ± 0.03[a,b]	2.39 ± 0.47	2.35±0.32

[a]Represents *P*<0.05 compared with the cortex by t test; b represents *P*<0.05 compared with the non-AKI group by t test

Table 10: Comparison of ROC curve analysis results of each positive parameter of IVIM, DTI, and DKI.

Index	AUC (0.95 CI)	Theoretical threshold	Sensitivity	Specificity	Youden index
Medulla fast ADC	0.682 (0.469~0.991)	17.0	0.704	0.671	0.385
Medulla Ff ADC	0.705 (0.564~0.881)	0.24	0.702	0.706	0.408
DTI cortex FA	0.728 (0.550~0.963)	0.26	0.748	0.704	0.452
DTI medulla FA	0.755 (0.592~0.962)	0.50	0.764	0.751	0.515
Medulla MK	0.804 (0.714~0.906)	0.44	0.793	0.818	0.611

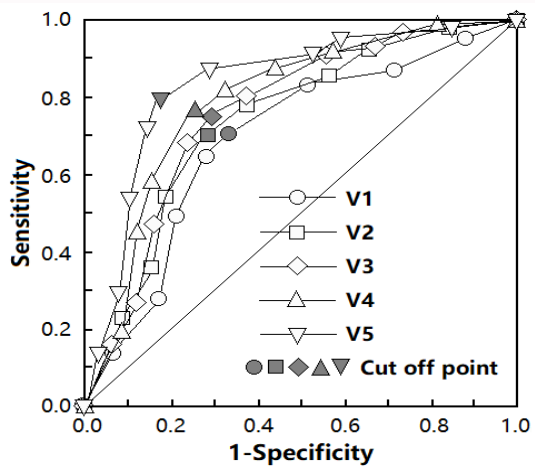

Figure 6: ROC curve analysis results of each positive parameter of IVIM, DTI, and DKI. V1: Medulla fast ADC, V2: Medulla Ff ADC, V3: DTI cortex FA, V4: DTI medulla FA, V5: Medulla MK.

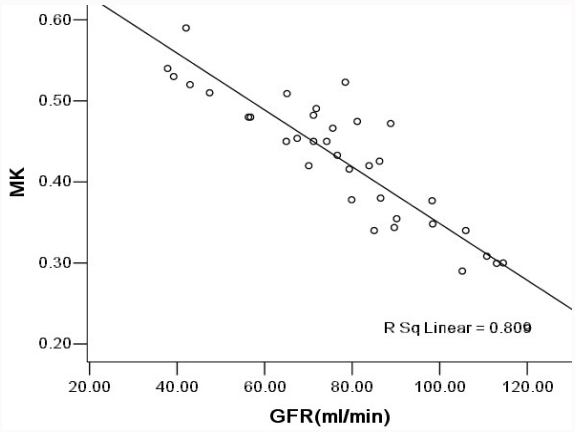

Figure 7: Correlation analysis between MK value and eGFR.

Regression analysis

Univariate logistic regression analysis showed that sex (OR=0.316, *P*=0.048), CHE (OR=0.886, *P*=0.003), eGFR (OR=0.865, *P*=0.005), BUN (OR=1.049, *P*=0.001), CR (OR=1.202, *P*=0.001), UA (OR=1.006, *P*=0.002), FA value (OR=0.999, *P*=0.001), percentage of CD3+ CD4+ T cells (OR=1.448, *P*=0.001), $CD4^+/CD8^+$ ratio (OR=1.203, *P*=0.001) and MK value (OR=1.554, *P*=0.001) were important predictors of AKI in acute pancreatitis. After further multivariate logistic regression analysis, we found that the percentage of CD3+ CD4+ T cells (OR=1.312, *P*=0.001), $CD4^+/CD8^+$ ratio (OR=1.256, *P*=0.001), and MK value (OR=1.530, *P*=0.001) were independent risk factors for acute pancreatitis with AKI.

Discussion

Important clinical indicators for predicting AKI in acute pancreatitis

AKI is a clinical syndrome defined as a sudden (within 48 h) and persistent decline in renal function caused by a variety of factors, including renal hypoperfusion, nephrotoxic substances, inflammatory factors, and urinary tract obstruction. At present, there are still no specific clinical treatment measures, and the mortality rate remains high. AKI is one of the common complications of acute pancreatitis, and its morbidity is between 1% and 14%, while the mortality rate of acute pancreatitis combined with AKI is between 0% and 30% [5,8,26]. However, a study found that of 414 SAP patients in the Intensive Care Unit (ICU), 287 (69.3%) developed AKI. In this study, 25% of SAP patients (14/56) developed AKI, which is consistent with the KDIGO guidelines. The proportion of men with AKI was higher than that of women (28.6% *vs.* 19.0%). This result is consistent with previous reports, indicating that male patients with acute pancreatitis are more likely to develop AKI.

Renal injury in AP is a complex disease caused by multiple factors, and various factors induce kidney injury through mutual intersection in the process of disease occurrence and development. Therefore, it is particularly important to discover multiple new molecular markers to realize the early prediction of AKI. In our study, there were no differences in liver function indices (TP, ALB, GLOB, TBIL, DBIL, TBA, ALT, AST, GGT and ALP) between AKI and non-AKI groups in SAP patients. These results suggested that liver function indicators should not be used to predict AKI in AP patients. In addition, blood urea nitrogen, creatinine, and uric acid levels were significantly increased in AKI patients, while serum LIP, CHE, and eGFR were decreased, which indicated that AP patients with AKI have severe renal damage. Univariate regression analysis showed that these variables may be important indicators for predicting AKI in acute pancreatitis.

The value of T lymphocyte subsets in the prediction and diagnosis of AKI in acute pancreatitis

The T lymphocyte subset is an important part of the body's

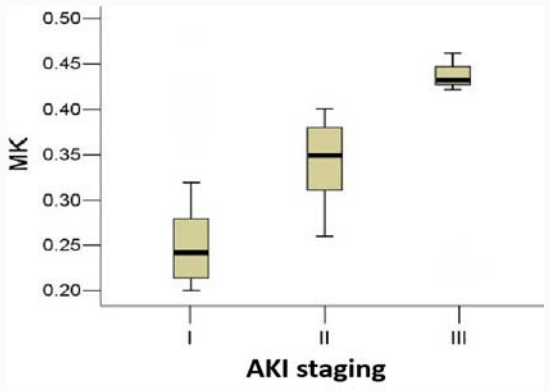

Figure 8: Comparison of renal medullary MK values in AKI patients at different stages.

immune system. Studies have shown that an imbalance in their proportion may lead to necrosis, infection and even death in AP patients [27]. In this study, we found that the percentage of CD3+ CD4+ T cells and the ratio of CD4+/CD8+ in peripheral blood in the AKI group were significantly lower than those in the non-AKI group, suggesting that the body exhibits immunosuppression in SAP patients. This result was consistent with previous reports. Therefore, our results showed that immunosuppression can occur in SAP patients at an early stage, and the decrease in the percentage of CD3+ CD4+ T cells and CD4+/CD8+ ratio could indicate the possibility of exacerbation of SAP patients with AKI.

Research value of IVIM, DTI, and DKI in acute pancreatitis with AKI

At present, blood Cr, BUN and urine volume is often used to evaluate renal function. However, the early diagnostic value of these indices is extremely limited, and they are vulnerable to some non-renal factors [28-30]. However, renal function MR imaging has become a hot topic in kidney research [31-35]. Kidney DTI studies are mainly used for the evaluation of renal pelvic ureter obstruction in children [36], diabetic nephropathy [37], polycystic kidney disease in children and adults [38], and ischemia- reperfusion injury of transplanted kidneys [39]. Renal IVIM research reports are mainly used for the identification of renal tumors [40-42] and the assessment of renal function damage caused by different reasons [43-45]. There are several reports on the application of DKI technology in the kidney [18,20,45,46]. In addition, our previous clinical studies have confirmed the value of DTI in the quantitative diagnosis and severity assessment of AP. Therefore, we attempted to apply multimodal DWI technologies to the further assessment of AKI in SAP patients.

In this study, to avoid the influence of cardiac motion on the image, we selected the right kidney as the parameter measurement object. Furthermore, many studies have confirmed that there is no significant difference in the FA, ADC, and MK parameters of the left and right kidneys [18,20,46]. Therefore, we have reason to believe that the right kidney can represent the body's renal function.

IVIM uses the observed signal attenuation of different b-values to determine renal microcirculation perfusion and diffusion, which can accurately reflect tissue DWI information. In this study, slow ADC values were not significantly different in the renal cortex and medulla, and there was still no difference between the two groups. However, the fast ADC and Ff ADC values of the renal medulla in the AKI group were significantly lower than those in the non-AKI group, and both of them had good diagnostic performance for AKI in SAP patients; the AUCs were 0.682 and 0.705, respectively. Moreover, the fast ADC values were moderately positively correlated with eGFR, which is consistent with research reports by Zhang et al. [47] and Liang et al. [48]. Our results indicate that renal microcirculation perfusion and effective blood flow are significantly reduced when SAP is combined with AKI. It is speculated that the causes are related to pathological changes, such as swelling and bleeding of glomerular cells, dysfunction of endothelial cells, increase in vascular permeability and infiltration of inflammatory cells.

The results of this study showed that the FA value of the renal cortex was significantly lower than that of the medulla in the DTI and DKI models, and the FA value of the renal parenchyma in AKI patients was lower than that in the control group and had good diagnostic performance for AKI in SAP patients. These results were inferred from two observations. On one hand, the kidney has a complex and special anatomical structure. The renal medulla, which consists of many blood vessels and straight tubules, is arranged in parallel and radial into the pelvis and sinus. The renal cortex is composed of many renal corpuscles and tubules, and the former is mainly composed of capillary globules distributed tortuously. It is precisely because of the difference in the microstructure of the renal cortex and medulla that the diffusion of water molecules in the renal medulla is more directional. On the other hand, when SAP is combined with AKI, pathological changes, such as decreased renal microcirculation perfusion, renal tubular injury, and renal tubular fibrosis, will cause limitations in the multi-directional diffusion of water molecules; as a result, the difference in anisotropic diffusion is relatively reduced, and the FA value decreases. Our results are consistent with the results of previous studies [49-51], which confirmed that FA can reflect pathophysiological changes in early renal injury in SAP patients. Although the ADC value of the renal cortex medulla in SAP patients with AKI was lower than that in the non-AKI group, there was no significant difference in value between the two groups. This result indicates that FA values are more sensitive than ADC in detecting renal functional changes in SAP patients, and the results were also supported in subsequent studies on the correlation between the FA values of the renal cortex and medulla and eGFR (r=0.696 and 0.689).

MK is the characteristic index of DKI, which reflects the average level of complexity of organizational structure in each direction. The MK value increases as the tissue complexity increases. In this study, we found that the MK value in the renal cortex in SAP patients was lower than that in the medulla, while the MK value in the renal medulla of AKI patients was significantly higher than that in the control group ($P<0.001$). We speculate that this may be related to the complex tubular structure of the renal medulla. In addition, when SAP is combined with AKI, pathological changes, such as swelling, necrosis and shedding of renal tubular epithelial cells; narrowing or occlusion of the official cavity; formation of an intracavitary tube type; infiltration of a large number of inflammatory cells; and a decrease in extracellular space, lead to an increase in the complexity of renal tissue. Therefore, MK is eventually increased. Moreover, we found that the renal medulla MK was negatively correlated with eGFR and positively correlated with AKI stage, which had the best diagnostic performance for AKI. Similarly, Mao et al. [46] found that renal parenchymal MK was negatively correlated with eGFR in chronic kidney disease. Therefore, our results showed that the MK value might be a supplementary indicator for diagnosing and determining the severity of kidney injury in SAP patients.

Correlation analysis

In this study, we found that eGFR was negatively correlated with renal medulla MK and positively correlated with the percentage of CD3+ CD4+ T cells and the CD4+/CD8+ ratio. Multivariate logistic regression analysis showed that the renal medulla MK value, percentage of CD3+ CD4+ T cells and CD4+/CD8+ ratio were independent risk factors for SAP patients with AKI. Therefore, using DKI combined with T lymphocyte subsets to determine the stage of renal injury in SAP patients may contribute to the diagnosis of AKI before eGFR reduction and provide the possibility for early intervention.

Research limitations

The number of SAP patients with AKI 25% (14/56) may have introduced a slight bias into our results. Moreover, SAP patients are in serious condition and have poor compliance in MR examination, which can affect image quality. Therefore, more patient data will be included in our future study.

Conclusion

In conclusion, the kidney IVIM, DTI and DKI parameters in the kidney had good early diagnostic value for AKI in SAP patients, especially the MK value of the renal medulla, which was positively correlated with AKI staging and negatively correlated with the eGFR. The decrease in the percentage of CD3+ CD4+ T cells and the $CD4^+$/$CD8^+$ ratio in peripheral blood indicate immunosuppression, which underscores the possibility of exacerbation of SAP patients with AKI. Therefore, the measurement of renal DKI parameters combined with $CD4^+$ T lymphocytes is practical for early diagnosis and predicting the severity of renal injury in SAP patients.

Acknowledgement

This study was supported by grants from the Project of Nanchong City School Cooperative Scientific Research (19SXHZ 0287) and the Scientific Research Project of Affiliated Hospital of North Sichuan Medical College (2020ZD013).

References

1. Kumar R, Pahwa N, Jain N. Acute kidney injury in severe acute pancreatitis: An experience from a tertiary care center. Saudi J Kidney Dis Transpl. 2015;26(1):56-60.
2. Zhou J, Li Y, Tang Y, Liu F, Yu S, Zhang L, et al. Effect of acute kidney injury on mortality and hospital stay in patient with severe acute pancreatitis. Nephrology (Carlton). 2015;20(7):485-91.
3. Li H, Qian Z, Liu Z, Liu X, Han X, Kang H. Risk factors and outcome of acute renal failure in patients with severe acute pancreatitis. J Crit Care. 2010;25(2):225-9.
4. Herrera GM, Seller PG, de La Rubia DGC, Chaparro Sanchez MJ, Nacle Lopez B. [Acute renal failure profile and prognostic value in severe acute pancreatitis]. Med Clin (Barc). 2000;115(19):721-5.
5. Wen X, Murugan R, Peng Z, Kellum JA. Pathophysiology of acute kidney injury: A new perspective. Contrib Nephrol. 2010;165:39-45.
6. Bansal S, Patel RN. Pathophysiology of contrast-induced acute kidney injury. Interv Cardiol Clin. 2020;9(3):293-8.
7. Vlachopanos G, Schizas D, Hasemaki N, Georgalis A. Pathophysiology of Contrast-Induced Acute Kidney Injury (CIAKI). Curr Pharm Des. 2019;25(44):4642-7.
8. Coca SG, Yalavarthy R, Concato J, Parikh CR. Biomarkers for the diagnosis and risk stratification of acute kidney injury: A systematic review. Kidney Int. 2008;73(9):1008-16.
9. Hui ES, Cheung MM, Qi L, Wu EX. Towards better MR characterization of neural tissues using directional diffusion kurtosis analysis. Neuroimage. 2008;42(1):122-34.
10. Cheung MM, Hui ES, Chan KC, Helpern JA, Qi L, Wu EX. Does diffusion kurtosis imaging lead to better neural tissue characterization? A rodent brain maturation study. Neuroimage. 2009;45(2):386-92.
11. Le Bihan D, Breton E, Lallem D, Aubin M L, Vignaud J, Laval-Jeantet M. Separation of diffusion and perfusion in intravoxel incoherent motion MR imaging. Radiology. 1988;168(2):497-505.
12. Basser PJ, Mattiello J, LeBihan D. MR diffusion tensor spectroscopy and imaging. Biophys J. 1994;66(1):259-67.
13. Li X, Liang Q, Zhuang L, Zhang X, Chen T, Li L, et al. Preliminary study of MR diffusion tensor imaging of the liver for the diagnosis of hepatocellular carcinoma. PLoS One. 2015;10(8):e0135568.
14. Li X, Zhuang L, Zhang X, Wang J, Chen T, Li L, et al. Preliminary study of MR diffusion tensor imaging of pancreas for the diagnosis of acute pancreatitis. PLoS One. 2016;11(9):e160115.
15. Collier Q, Veraart J, Jeurissen B, Vanhevel F, Pullens P, Parizel PM, et al. Diffusion kurtosis imaging with free water elimination: A Bayesian estimation approach. Magn Reson Med. 2018;80(2):802-813.
16. Yan X, Zhou M, Ying L, Yin D, Fan M, Yang G, et al. Evaluation of optimized b-value sampling schemas for diffusion kurtosis imaging with an application to stroke patient data. Comput Med Imaging Graph. 2013;37(4):272-80.
17. Poot DH, den Dekker AJ, Achten E, Verhoye M, Sijbers J. Optimal experimental design for diffusion kurtosis imaging. IEEE Trans Med Imaging. 2010;29(3):819-29.
18. Pentang G, Lanzman RS, Heusch P, Muller-Lutz A, Blondin D, Antoch G. Diffusion kurtosis imaging of the human kidney: A feasibility study. Magn Reson Imaging. 2014;32(5):413-20.
19. Zhao J, Wang ZJ, Liu M, Zhu J, Zhang X, Zhang T, et al. Assessment of renal fibrosis in chronic kidney disease using diffusion-weighted MRI. Clin Radiol. 2014;69(11):1117-22.
20. Huang Y, Chen X, Zhang Z, Yan L, Pan D, Liang C, et al. MRI quantification of non-Gaussian water diffusion in normal human kidney: A diffusional kurtosis imaging study. NMR Biomed. 2015;28(2):154-61.
21. Banks PA, Bollen TL, Dervenis C, Gooszen HG, Johnson CD, Sarr MG, et al. Classification of acute pancreatitis--2012: Revision of the Atlanta classification and definitions by international consensus. Gut. 2013;62(1):102-111.
22. Carioca AL, Jozala DR, de Bem LO, Rodrigues JM. Severity assessment of acute pancreatitis: Applying Marshall scoring system. Rev Col Bras Cir. 2015;42(5):325-7.
23. Gordon CE, Balk EM, Francis JM. Summary of the 2018 Kidney Disease Improving Global Outcomes (KDIGO) Guideline on hepatitis C in chronic kidney disease. Semin Dial. 2019;32(2):187-95.
24. Tabesh A, Jensen JH, Ardekani BA, Helpern JA. Estimation of tensors and tensor-derived measures in diffusional kurtosis imaging. Magn Reson Med. 2011;65(3):823-36.
25. Xie CL, Zhang M, Chen Y, Hu R, Tang MY, Chen TW, et al. Spleen and splenic vascular involvement in acute pancreatitis: An MRI study. Quant Imaging Med Surg. 2018;8(3):291-300.
26. Srisawat N, Kellum JA. Acute kidney injury: Definition, epidemiology, and outcome. Curr Opin Crit Care. 2011;17(6):548-55.
27. Yu ZX, Chen XC, Zhang BY, Liu N, Gu Q. Association between HLA-DR Expression and multidrug-resistant infection in patients with severe acute pancreatitis. Curr Med Sci. 2018;38(3):449-54.

28. Yang N, Li B, Ye B, Ke L, Chen F, Lu G, et al. The long-term quality of life in patients with persistent inflammation-immunosuppression and catabolism syndrome after severe acute pancreatitis: A retrospective cohort study. J Crit Care. 2017;42:101-6.

29. Kylanpaa ML, Repo H, Puolakkainen PA. Inflammation and immunosuppression in severe acute pancreatitis. World J Gastroenterol. 2010;16(23):2867-72.

30. Ueda T, Takeyama Y, Yasuda T, Shinzeki M, Sawa H, Nakajima T, et al. Immunosuppression in patients with severe acute pancreatitis. J Gastroenterol. 2006;41(8):779-84.

31. Schneider AG, Goodwin MD, Bellomo R. Measurement of kidney perfusion in critically ill patients. Crit Care. 2013;17(2):220.

32. Prevost VH, Girard OM, Callot V, Cozzone PJ, Duhamel G. Fast imaging strategies for mouse kidney perfusion measurement with pseudocontinuous Arterial Spin Labeling (pCASL) at ultra high magnetic field (11.75 tesla). J Magn Reson Imaging. 2015;42(4):999-1008.

33. Hilbert F, Bock M, Neubauer H, Veldhoen S, Wech T, Bley TA, et al. An intravoxel oriented flow model for diffusion-weighted imaging of the kidney. NMR Biomed. 2016;29(10):1403-13.

34. Mahmoud H, Buchanan C, Francis ST, Selby NM. Imaging the kidney using magnetic resonance techniques: Structure to function. Curr Opin Nephrol Hypertens. 2016;25(6):487-93.

35. Xie L, Bennett KM, Liu C, Johnson GA, Zhang JL, Lee VS. MRI tools for assessment of microstructure and nephron function of the kidney. Am J Physiol Renal Physiol. 2016;311(6):F1109-24.

36. Otero HJ, Calle-Toro JS, Maya CL, Darge K, Serai SD. DTI of the kidney in children: Comparison between normal kidneys and those with Ureteropelvic Junction (UPJ) obstruction. MAGMA. 2020;33(1):63-71.

37. Deng Y, Yang BR, Luo JW, Du GX, Luo LP. DTI-based radiomics signature for the detection of early diabetic kidney damage. Abdom Radiol (NY). 2020;45(8):2526-31.

38. Serai SD, Otero HJ, Calle-Toro JS, Berman JI, Darge K, Hartung EA. Diffusion tensor imaging of the kidney in healthy controls and in children and young adults with autosomal recessive polycystic kidney disease. Abdom Radiol (NY). 2019;44(5):1867-72.

39. Jager KJ, Stel VS, Branger P, Guijt M, Busic M, Dragovic M, et al. The effect of differing kidney disease treatment modalities and organ donation and transplantation practices on health expenditure and patient outcomes. Nephrol Dial Transplant. 2018;33(4):560-2.

40. Rheinheimer S, Stieltjes B, Schneider F, Simon D, Pahernik S, Kauczor HU, et al. Investigation of renal lesions by diffusion-weighted magnetic resonance imaging applying intravoxel incoherent motion-derived parameters--initial experience. Eur J Radiol. 2012;81(3):e310-6.

41. Gaing B, Sigmund EE, Huang WC, Babb JS, Parikh NS, Stoffel D, et al. Subtype differentiation of renal tumors using voxel-based histogram analysis of intravoxel incoherent motion parameters. Invest Radiol. 2015;50(3):144-52.

42. Ding Y, Zeng M, Rao S, Chen C, Fu C, Zhou J. Comparison of biexponential and monoexponential model of diffusion-weighted imaging for distinguishing between common renal cell carcinoma and fat poor angiomyolipoma. Korean J Radiol. 2016;17(6):853-63.

43. Xiong R, Li W, Li Y, Zheng K, Zhang T, Gao M, et al. Er Shen Wan extract reduces diarrhea and regulates AQP 4 and NHE 3 in a rat model of spleen-kidney Yang deficiency-induced diarrhea. Biomed Pharmacother. 2018;98:834-46.

44. Kim JW, Lee CH, Yoo KH, Je BK, Kiefer B, Park YS, et al. Intravoxel incoherent motion magnetic resonance imaging to predict vesicoureteral reflux in children with urinary tract infection. Eur Radiol. 2016;26(6):1670-7.

45. Ebrahimi B, Rihal N, Woollard JR, Krier JD, Eirin A, Lerman LO. Assessment of renal artery stenosis using intravoxel incoherent motion diffusion-weighted magnetic resonance imaging analysis. Invest Radiol. 2014;49(10):640-6.

46. Mao W, Ding Y, Ding X, Wang Y, Fu C, Zeng M, et al. Pathological assessment of chronic kidney disease with DWI: Is there an added value for diffusion kurtosis imaging? J Magn Reson Imaging. 2021;54(2):508-517.

47. Zhang B, Dong Y, Guo B, Chen W, Ouyang F, Lian Z, et al. Application of noninvasive functional imaging to monitor the progressive changes in kidney diffusion and perfusion in contrast-induced acute kidney injury rats at 3.0 T. Abdom Radiol (NY). 2018;43(3):655-62.

48. Liang L, Chen WB, Chan KW, Li YG, Zhang B, Liang CH, et al. Using intravoxel incoherent motion MR imaging to study the renal pathophysiological process of contrast-induced acute kidney injury in rats: Comparison with conventional DWI and arterial spin labeling. Eur Radiol. 2016;26(6):1597-605.

49. Feng YZ, Ye YJ, Cheng ZY, Hu JJ, Zhang CB, Qian L, et al. Non-invasive assessment of early stage diabetic nephropathy by DTI and BOLD MRI. Br J Radiol. 2020;93(1105):20190562.

50. Ye XJ, Cui SH, Song JW, Liu K, Huang XY, Wang L, et al. Using magnetic resonance diffusion tensor imaging to evaluate renal function changes in diabetic patients with early-stage chronic kidney disease. Clin Radiol. 2019;74(2):116-22.

51. Hueper K, Hartung D, Gutberlet M, Gueler F, Sann H, Husen B, et al. Magnetic resonance diffusion tensor imaging for evaluation of histopathological changes in a rat model of diabetic nephropathy. Invest Radiol. 2012;47(7):430-7.